Int. J. Heat Mass Transfer. Vol. 26, No. 9, pp. 1265–1273, 1983
Printed in Great Britain

0017-9310/83 $3.00 + 0.00

HYDRODYNAMICS AND HEAT TRANSFER IN SPHERE ASSEMBLAGES—CYLINDRICAL CELL MODELS

R. TAL (THAU),* D. N. LEE† and W. A. SIRIGNANO‡

* Dept. of Mechanical Engineering, † Dept. of Mathematics and ‡ Dept. of Mechanical Engineering, Carnegie-Mellon University, Pittsburgh, PA 15213, U.S.A.

(*Received* 29 *March* 1982 *and in revised form on* 3 *December* 1982)

Abstract—In order to evaluate interactions between vaporizing fuel droplets, a cylindrical cell model based on a single sphere has been suggested by the authors in previous works as a replacement for the existing spherical cell model. Since wake effects are important, a multisphere cylindrical cell model has been developed in the present work. The Navier–Stokes and energy equations have been solved numerically within the representative cells for intermediate Reynolds numbers. Using a nonuniform mesh suited for the problem, several spheres in tandem are considered and the importance of wake effects in considerably reducing the drag and Nusselt number in the bulk is discussed. The quasiperiodic features of the results are indicated and compared favorably with a model assuming periodicity *a priori*.

NOMENCLATURE

a, radius of sphere in array;
A, increment in the positive x direction;
b, half distance between sphere centers in array;
B, increment in the negative x direction;
C, increment in the positive y direction;
c_d, total drag coefficient;
c_{df}, friction drag coefficient;
c_{dp}, pressure drag coefficient;
D, increment in the negative y direction;
h, heat transfer coefficient;
K_H, thermal diffusivity;
Nu, Nusselt number, $2ah/K_H$;
n, normal to the surface;
Pr, Prandtl number, $c_p\mu/K_H$;
Re, Reynolds number, $2aV_\infty/K_H$;
T, dimensionless temperature, $(T'-T'_0)/(T'_\infty-T'_0)$;
T_{wall}, dimensionless wall temperature;
$\bar{T}(x)$, average temperature at cross-section x;
T', temperature;
T'_0, surface temperature;
T'_∞, inlet temperature;
U, scaled dimensionless vorticity;
u, velocity component in the x direction;
V_∞, inlet velocity;
x, axial coordinate in cylindrical polar system;
y, radius in cylindrical polar coordinate system.

Greek symbols

θ, scaled temperature function;
μ, viscosity;
ψ, dimensionless stream-function, $\psi'/V_\infty a^2$;
ν, kinematic viscosity;
ω, dimensionless vorticity, $\omega' a/V_\infty$.

INTRODUCTION

THE VAPORIZATION of liquid fuels is an important combustion problem since in many practical situations, vaporization can be the rate-controlling phenomenon. Real liquid spray behavior is quite complicated. Important effects include: relative motion between gas and droplet leading to convective heating and internal circulation, transient heating of the liquid, droplet–droplet interactions, droplet–turbulent eddy interactions, and multicomponent liquid behavior. The present analysis is intended to concentrate on droplet–droplet interactions with convective heating in a steady-state situation. Among other items, mass transfer and vaporization, internal circulation, and transient heating will not be considered. Rather an idealized array of constant diameter spheres will be examined with the intention to understand the hydrodynamics and convective heating. Clearly, such a basic understanding is vital to the combustion field but also applies to many other problems.

A non-steady state solution for the problem of droplet vaporization at intermediate Reynolds numbers, featuring the effects of internal circulation, was developed by Prakash and Sirignano [1, 2] and Lara-Urbaneja and Sirignano [3]. This solution is limited to a single droplet, while Chigier [4] in a review paper indicated that individual droplet combustion is rare in practical systems. Nevertheless, most studies on the combustion of atomized fuel consider the burning of individual droplets and relatively few works have been done on interactions between droplets. This point is most evident in an extensive review by Faeth [5].

Fedoseeva [6] and Twardus and Brzustowski [7] used bispherical coordinates for calculating the interactions between vaporizing and burning droplets. Labowsky [8, 9], Labowsky and Rosner [10], Fedoseeva [11], Fedoseeva *et al.* [12], Ray and Davis [13] and Chiu and Liu [14] addressed the problem of transfer rate calculations in arrays of interacting droplets. All of the above-mentioned studies of droplet interactions were limited to quiescent environments, thus being diffusion analyses.

In real combustors, the Reynolds number based on fuel droplet diameter can be as high as 200, thus indicating that a diffusion-only analysis of interactions between vaporizing droplets should be inadequate. For

that reason, an analysis for vaporization of interacting droplets is being developed. The interactions between droplets in an assemblage stem from modified boundary conditions of the continuous (gas) phase, the disperse (liquid) phase being influenced through interface boundary conditions. Therefore, the continuous phase solution is presently pursued, and will be later coupled with existing or on-going liquid phase solutions [1, 2, 28]. A cylindrical cell model for the hydrodynamics of sphere assemblages at intermediate Reynolds numbers was developed by Tal and Sirignano [15]. This model provided significant improvement in compliance with experimental results as compared to the spherical cell model first applied to the range of intermediate Reynolds numbers by LeClair and Hamielec [17]. Besides its quantitative advantage, the cylindrical cell model is physically more meaningful, as it distinguishes between the streamwise and cross-stream directions in formulating the problem. The cylindrical cell model has been also used by Tal and Sirignano [18] for numerical heat transfer calculations in an assemblage of spheres at intermediate Reynolds numbers. An interaction parameter has been defined and found to be quite independent of the Reynolds and Prandtl numbers. The Nusselt numbers calculated were found to be closer to experimental results [19] than previous analyses by LeClair and Hamielec [20] and Woo [21] based on the spherical cell model. Notwithstanding the reasonable agreement between calculated and experimental data, this comparison has been done only for average values. Experimental data for velocity distribution and local heat transfer rates in assemblages are unavailable. The most important limitation of both the spherical and cylindrical cell models is that some assumption is necessary for the values of the vorticity, stream-function and temperature on the cell boundaries. For example, the breakdown of the assumption of zero vorticity is reported by Akiyama *et al.* [22] for a Reynolds number of above 70, indicating the importance of wake effects. In fact the multisphere problem is truly elliptic and, for that reason, it should be solved as an entity. However, it is realized that such a 3-dim. solution is presently not feasible without some idealization. In order to estimate the amount of idealization involved in using a single-sphere cell and especially the wake effects, a study of multisphere cells is undertaken in this paper.

MATHEMATICAL FORMULATION OF THE PROBLEM

We consider an infinite array of spheres of radius a with a uniform spacing $2b$ (Fig. 1). Due to symmetry and the nearly periodic character associated with an infinite array we assume no heat transfer or momentum transfer takes place at the streamwise equidistant planes between the spheres. By this assumption, the problem is reduced to a multitude of spheres in tandem in a square streamtube (Fig. 2). As this is clearly a 3-dim. problem and appears to be intractable even with the latest numerical techniques, we replace the square duct with a cylindrical duct of equal cross-section. As all the length dimensions will be expressed in a dimensionless form based on the sphere radius a, the cylindrical cell radius is $(b/a)(4/\pi)^{1/2}$. Clearly, the void fraction of the cylindrical cell is equal to the void fraction of the whole assemblage.

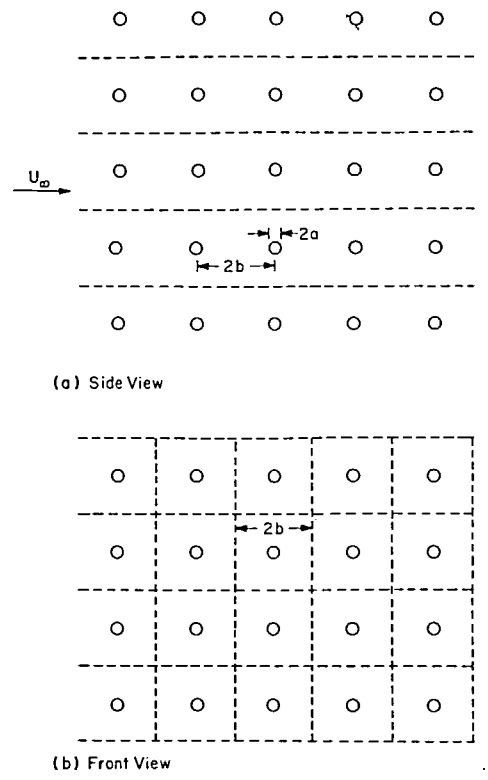

FIG. 1. Assemblage geometry. (a) Side view. (b) Front view.

The governing differential equations for the flow field and heat transfer in cylindrical polar coordinates are:

(a) The Navier–Stokes equations in vorticity stream function formulation,

$$U = \frac{\partial^2 \psi}{\partial x^2} + \frac{\partial^2 \psi}{\partial y^2} - \frac{1}{y}\frac{\partial \psi}{\partial y}, \tag{1}$$

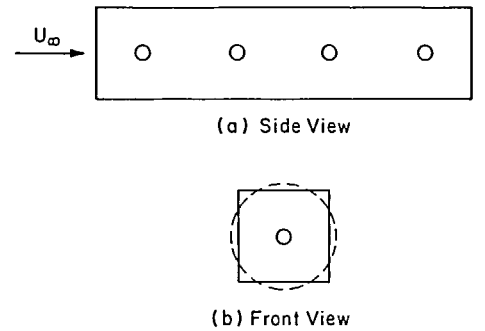

FIG. 2. Multisphere cylindrical cell. (a) Side view. (b) Front view.

$$\frac{Re}{2y}\left[\frac{\partial\psi}{\partial y}\frac{\partial U}{\partial x}-\frac{\partial\psi}{\partial x}\frac{\partial U}{\partial y}\right]+\frac{ReU}{y^2}\frac{\partial\psi}{\partial x}=\frac{\partial^2 U}{\partial x^2}+\frac{\partial^2 U}{\partial y^2}-\frac{1}{y}\frac{\partial U}{\partial y} \quad (2)$$

with U being defined as ωy.

(b) The energy equation,

$$\frac{Re\,Pr}{2y}\left[\frac{\partial\psi}{\partial y}\frac{\partial T}{\partial x}-\frac{\partial\psi}{\partial x}\frac{\partial T}{\partial y}\right]=\frac{\partial^2 T}{\partial x^2}+\frac{\partial^2 T}{\partial y^2}+\frac{1}{y}\frac{\partial T}{\partial y} \quad (3)$$

with Reynolds and Prandtl numbers defined as

$$Re=\frac{2V_\infty a}{\nu}, \quad (4)$$

$$Pr=\frac{c_p\mu}{K_H}. \quad (5)$$

U, ψ, T and y are dimensionless variables.

The boundary conditions for the cylindrical cell model are:

(a) At the inlet:

$$\psi=\tfrac{1}{2}y^2, \quad (6)$$

$$\omega=0, \quad (7)$$

$$T=1. \quad (8)$$

(uniform flow).

(b) At the outlet

$$\frac{\partial\psi}{\partial x}=0, \quad (9)$$

$$\frac{\partial\omega}{\partial x}=0, \quad (10)$$

$$\frac{\partial T}{\partial x}=0. \quad (11)$$

(c) On the sphere surfaces

$$\psi=0, \quad (12)$$

$$\frac{\partial\psi}{\partial n}=0, \quad (13)$$

$$T=0. \quad (14)$$

(The vorticity boundary conditions are calculated by using the two stream-function boundary conditions.)

(d) Along the axis of symmetry

$$\psi=0, \quad (15)$$

$$\omega=0, \quad (16)$$

$$\frac{\partial T}{\partial y}=0. \quad (17)$$

(e) On the cylindrical cell envelope

$$\psi=\frac{2}{\pi}(b/a)^2, \quad (18)$$

$$\omega=0, \quad (19)$$

$$\frac{\partial T}{\partial y}=0. \quad (20)$$

(The basic idea in solving the system of equations for a multisphere cell is that the upstream and downstream boundary conditions might affect the spheres closer to the inlet or to the outlet, but the spheres in the bulk would be less affected by the type of boundary conditions used.)

FINITE DIFFERENCE FORMULATION AND SOLUTION PROCEDURE

For the numerical solution of the problem, it is important to select a mesh which enables a convenient expression to be obtained for the boundary conditions. For this reason, we select a nonuniform cylindrical polar mesh. The basic unit of the cell geometry, including 55 × 23 points, is shown in Fig. 3, and this unit can be extended in the streamwise direction, thus generating a multisphere cell. The important factors of this coordinate system are:

(1) orthogonality;

(2) the coordinate lines are parallel or perpendicular to the cell boundaries;

(3) the sphere surface, even not including constant-

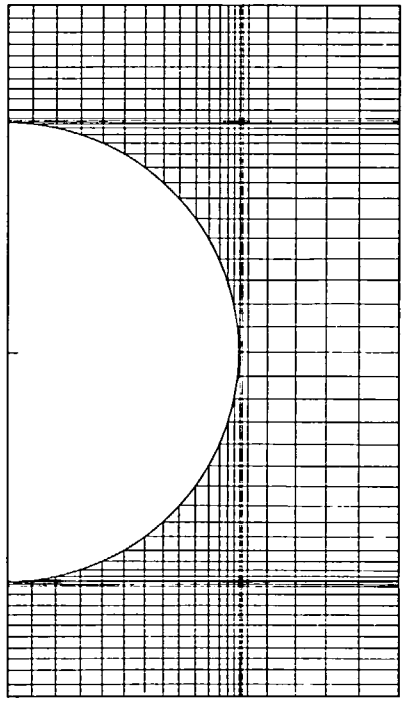

FIG. 3. Nonuniform mesh geometry.

coordinate lines, passes through grid points only, not intersecting the mesh lines elsewhere;

(4) the mesh is fine near the surface and coarse elsewhere.

The partial derivatives of any function F appearing in the differential equations are expressed in a divided difference form [23] for a nonuniform grid based on the following expression:

$$\left.\frac{\partial F}{\partial x}\right|_{ij} = \frac{(A^2-B^2)F_{ij}+B^2F_{i+1,j}-A^2F_{i-1,j}}{AB(A+B)}, \quad (21)$$

$$\left.\frac{\partial F}{\partial y}\right|_{ij} = \frac{(C^2-D^2)F_{i,j}+D^2F_{i,j+1}-C^2F_{i,j-1}}{CD(C+D)}, \quad (22)$$

$$\left.\frac{\partial^2 F}{\partial x^2}\right|_{ij} = \frac{2BF_{i+1,j}+2AF_{i-1,j}-2(A+B)F_{ij}}{AB(A+B)}, \quad (23)$$

$$\left.\frac{\partial^2 F}{\partial y^2}\right|_{ij} = \frac{2DF_{i,j+1}+2CF_{i,j-1}-2(C+D)F_{ij}}{CD(C+D)}. \quad (24)$$

Note that for a uniform grid, the above divided difference scheme reduces to the usual five point star difference scheme for the Laplace operator. The diffusion terms are expressed using a centered difference scheme and the convective terms (both in the vorticity and the energy equation) using an upwind difference scheme.

The nonlinear coupling of the stream-function equation and the vorticity equation was treated by pure iteration, i.e. first solved for stream-functions, then solved for vorticity and iterated, until a desired accuracy was reached. The matrix problem generated by the difference scheme for each variable is solved by matrix iteration. The adaptive successive over-relaxation (SOR) method is used for the stream-function equation. For the vorticity and temperature equations, a reduced system method with conjugate gradient acceleration is used, this also requires that the linear system be re-ordered into a "red-black" indexing [24].

RESULTS OF THE NUMERICAL SOLUTION

Constant property line plots

Two spacings have been evaluated at $Re = 100$ and $Pr = 1$: $b/a = 1.5$ and $b/a = 3.0$. The stream-function patterns, constant vorticity lines and isotherm patterns for a cylindrical cell containing three spheres are presented in Figs. 4 and 5. Note the qualitative periodicity evolving in some of the patterns, especially comparing the second and third sphere in each cell. A detailed quantitative estimate of the periodicity will be undertaken in the next section.

Evolution of periodic conditions

Comparing the values of the stream-function and of the vorticity at equidistant planes between the first and second spheres ($x = 3$ for $b/a = 1.5$) and the second and third sphere ($x = 6$ for the same b/a) we find a remarkable periodicity evolving already one sphere after the entrance section. There is virtually no change in the stream-function profile and only very little change in the vorticity profile (as vorticity is generated and diffused downstream) (Fig. 6).

As vorticity is related (approximately) to the second derivative of the stream-function, the slight changes in the stream-function curvature are equivalent to the changes in the vorticity profile. Based upon the vorticity pattern, it is believed that the changes would be even less significant at the following stages if the present model is applied for four or more spheres in a cell. (There is no limitation in our model for the number of successive spheres in the cell to be considered. However, because of practical considerations of computer time and storage, we limited the present study to three spheres in a cell.)

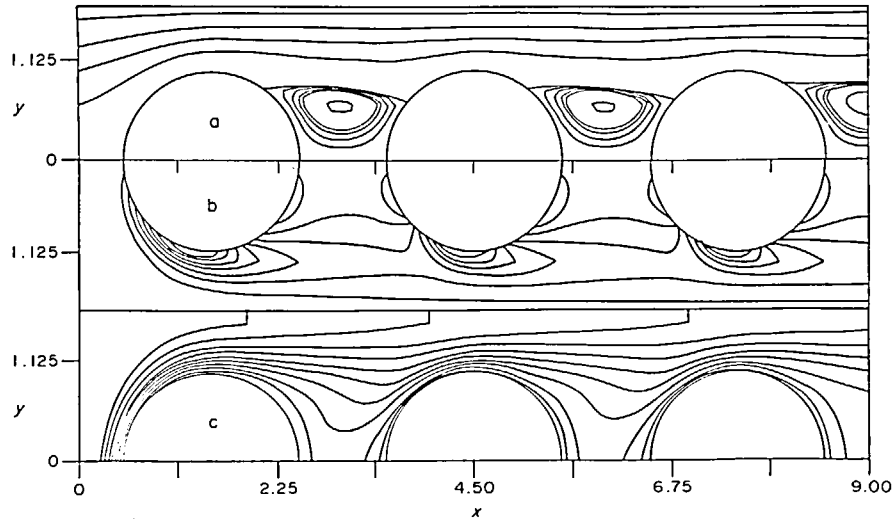

FIG. 4. Stream-function (a), vorticity (b) and isotherms (c) patterns for three spheres in a cell. $b/a = 1.5$, $Re = 100$, $Pr = 1$.

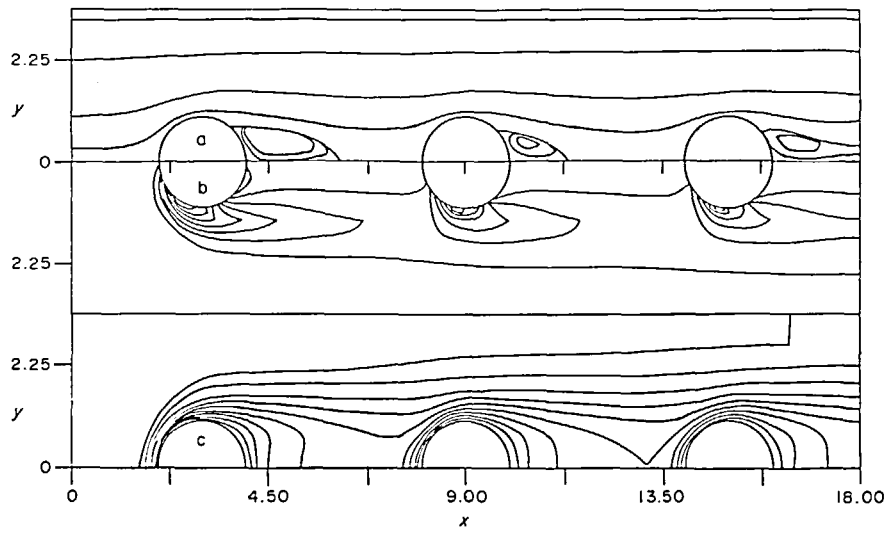

FIG. 5. Stream-function (a), vorticity (b) and isotherms (c) patterns for three spheres in a cell. $b/a = 3.0$, $Re = 100$, $Pr = 1$.

Despite the similar shape of the isotherm patterns, periodicity was neither expected nor obtained for the temperature field. However, as indicated by Patankar *et al.* [25], for uniform wall temperature, profiles of similar shape recur periodically.

A sectional average temperature is defined as

$$\bar{T}(x)-T_{\text{wall}} = \frac{\int_{Y_{\min}}^{Y_{\max}} [T(x,y)-T_{\text{wall}}]|u|2\pi y \, dy}{\int_{Y_{\min}}^{Y_{\max}} |u|2\pi y \, dy}. \quad (25)$$

Note that T_{wall} is 0 by definition and will be dropped subsequently.

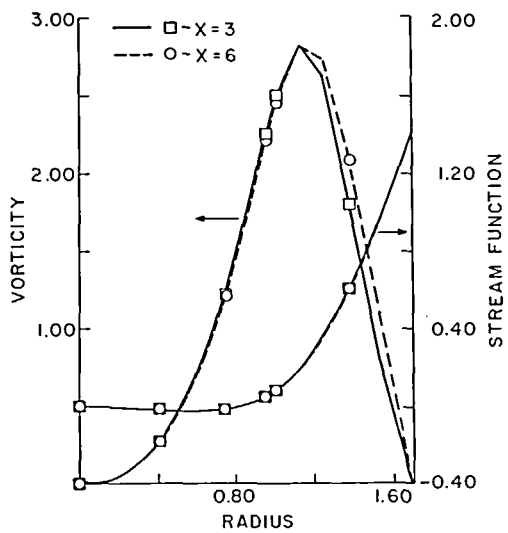

FIG. 6. Comparison of stream-function and vorticity values at $x = 3.0$ and $x = 6.0$. $Re = 100$, $b/a = 1.5$.

A scaled temperature function $\theta(x, y)$ is defined as

$$\theta(x,y) = \frac{T(x,y)-T_{\text{wall}}}{\bar{T}(x)-T_{\text{wall}}} = \frac{T(x,y)}{\bar{T}(x)}. \quad (26)$$

Obviously, $\theta(x, y)$ satisfies the condition

$$\frac{\int_{Y_{\min}}^{Y_{\max}} \theta(x,y)|u|2\pi y \, dy}{\int_{Y_{\min}}^{Y_{\max}} |u|2\pi y \, dy} = 1. \quad (27)$$

$\theta(x, y)$ has been calculated for $Re = 100$, $Pr = 1$, $b/a = 1.5$ and is presented in Fig. 7.

Comparing the values of $\theta(x, y)$ at $x = 3$ and $x = 6$ (Fig. 8) the quasi-periodicity of this function is established, without any *a priori* assumption.

Results based on assuming periodicity a priori

Patankar *et al.* [25] identified the periodicity characteristics of fully developed flow in ducts having streamwise-periodic variations of cross-sectional area. The geometry considered was a transverse plate array.

Knowing the evolution of periodic conditions in a multisphere cell and given the suggestions of Patankar *et al.* [25], we performed a numerical solution of the Navier–Stokes equations based upon a periodic boundary condition. The values of the stream-function and vorticity at the cell entrance and exit sections are assumed to be equal (but unknown). The other boundary conditions did not change and the equations were solved iteratively following the same numerical process as in the previous cases presented. Stream-function and vorticity patterns are given in Fig. 9.

The problem is more complicated for the energy equation. $T(x, y)$ is replaced by $\theta(x, y)\bar{T}(x)$ and the

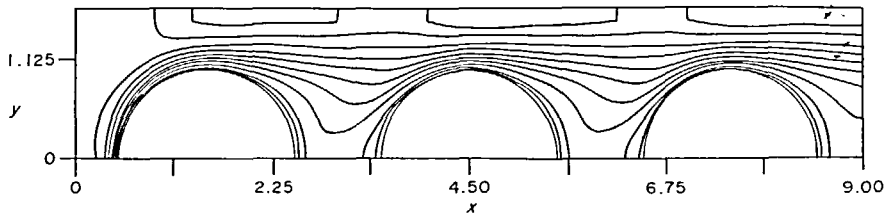

FIG. 7. θ function pattern for three spheres in a cell. $b/a = 3.0$, $Re = 100$, $Pr = 1.0$.

following non-homogeneous equation is obtained:

$$\frac{RePr}{2y}\left[\frac{\partial\psi}{\partial y}\frac{\partial\theta}{\partial x}-\frac{\partial\psi}{\partial x}\frac{\partial\theta}{\partial y}\right]-\left[\frac{\partial^2\theta}{\partial x^2}+\frac{\partial^2\theta}{\partial y^2}+\frac{1}{y}\frac{\partial\theta}{\partial y}\right]$$
$$=\frac{1}{\bar{T}(x)}\left[\theta\frac{d^2\bar{T}(x)}{dx^2}+\frac{d\bar{T}(x)}{dx}\left(2\frac{\partial\theta}{\partial x}-\frac{RePr}{2y}\frac{\partial\psi}{\partial y}\theta\right)\right]. \quad (28)$$

As $\theta(x, y)$ is assumed to be periodic, the RHS of the equation has to be periodic as well. Note that $\bar{T}(x)$ is an unknown function which has to be solved as an eigenvalue. The additional condition (27) can be used in the iterative process to identify the valid values of $\bar{T}(x)$. An iterative procedure for solving $\theta(x, y)$ for a periodic array of plates is presented by Patankar *et al.* [25]. In the present problem, a modified and significantly simpler version of the above-mentioned procedure was used. This procedure is presented in great detail elsewhere [26]. The isotherm pattern obtained in a representative cell, based on this procedure is given in Fig. 9. The quasi-periodic nature of the flow field as well as of the scaled temperature field are assessed in the next section, by comparing drag coefficients and Nusselt numbers for various situations.

Drag coefficients and Nusselt number results

The values of the drag coefficients and Nusselt numbers calculated using the multisphere cylindrical cell model and the periodic model are given in Tables 1 and 2. For the case of three spheres in a cell, the values are given in consecutive order. The periodic solution as well as the unconfined solution have to be compared with the values for the second sphere, which are the closest to the bulk values (the first sphere and the third sphere represent inlet and outlet conditions, respectively).

The conclusions of Patankar *et al.* [25] about periodicity of the temperature profiles are: (a) for modularly repeating wall heat flux, the temperature field is periodic after a linear term related to the bulk temperature change is subtracted; (b) for uniform wall temperature, profiles of similar shape recur periodically but the temperature field is not periodic. Our study assumed uniform temperature on the sphere surfaces and despite the apparently similar patterns of the isotherms (Figs. 4 and 5), periodicity was neither expected nor obtained, nor was a study assuming periodic boundary conditions performed. The quasi-

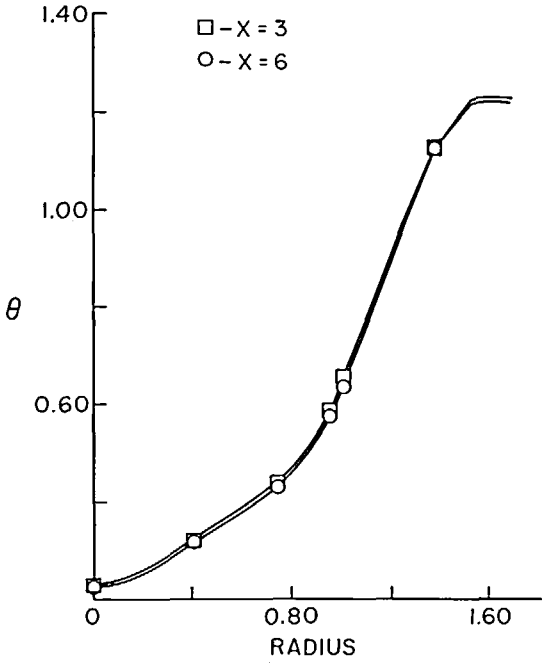

FIG. 8. Comparison of θ function values at $x = 3.0$ and $x = 6.0$. $Re = 100$, $b/a = 1.5$.

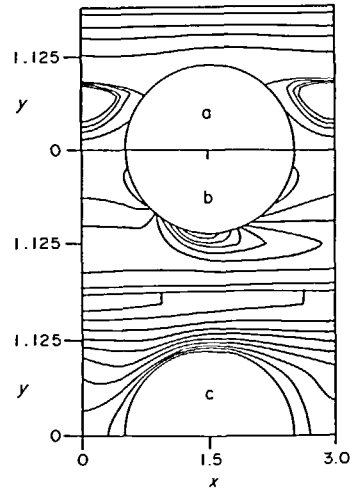

FIG. 9. Stream-function (a), vorticity (b) and isotherms (c) patterns assuming periodicity. $b/a = 1.5$, $Re = 100$, $Pr = 1$.

Table 1. Drag coefficients in cylindrical cells ($Re = 100$, $b/a = 1.5$)

Type of solution	c_{df}	c_{dp}	c_d
3 Spheres in a cell	0.966, 0.692, 0.677	0.977, 0.693, 0.671	1.964, 1.385, 1.349
Periodic	0.673	0.657	1.330
Unconfined	0.675	0.639	1.314

Table 2. Values of Nusselt number in cylindrical cells

Type of solution	Nu	Remarks
3 Spheres in a cell	7.644, 4.765, 4.061	Nu based on inlet to first sphere
3 Spheres in a cell	7.644, 6.151, 6.270	Nu based on inlet to each cell unit
Periodic	5.935	
Unconfined	7.910	

periodic nature of the flow field and the aperiodic nature of the temperature field will now be assessed, by comparing drag coefficients and Nusselt numbers for various situations.

The values of the drag coefficients calculated for several spheres in the cylindrical cell are summarized in Table 1. The values of c_{df}, c_{dp}, c_d, corresponding to the friction drag and total drag coefficients for the first sphere in the cell are considerably higher than for an unconfined sphere. This result is in compliance with previous studies of LeClair and Hamielec [17] and Tal and Sirignano [15]. The physical cause is increased shear stresses on the spheres and changes in the pressure distribution due to the acceleration of the flow as a result of lateral confinement. Wake effects are not present on the upstream hemisphere of the first sphere in the cell. For the following spheres in the cell, the wake of the previous sphere extends out to the upstream hemisphere, creating a low pressure region there. This effect reduces the pressure drag. In addition, the recirculating nature of the flow causes a reversal in the direction of the friction drag in the corresponding zone. The lateral confinement effects are still present for the second and third sphere in the cell, but they are limited to the non-recirculating zones and are almost offset by the longitudinal wake effects. It is evident that the periodic solution gives a very good approximation of the values of the drag coefficients for the second and third sphere in the cell. Furthermore, given the trend of a slight decrease in the drag coefficients between the second and third sphere, it is expected that the values for subsequent spheres would be even closer to the periodic values.

A comparison of the values of the average Nusselt number is given in Table 2. For the temperature field there are also two types of interaction between the spheres: lateral interactions, which tend to increase the Nusselt number and wake interactions, which tend to reduce the Nusselt number. On the first sphere in the row, these two types of interactions almost offset each other. On the following spheres in the row, the wake interactions are stronger than the lateral effects, and the forward stagnation region, which is in this case a slowly recirculating zone, is a low heat transfer rate region. The local Nusselt numbers for each of the three spheres in tandem are presented in Fig. 10, and the effect of the wakes is evident.

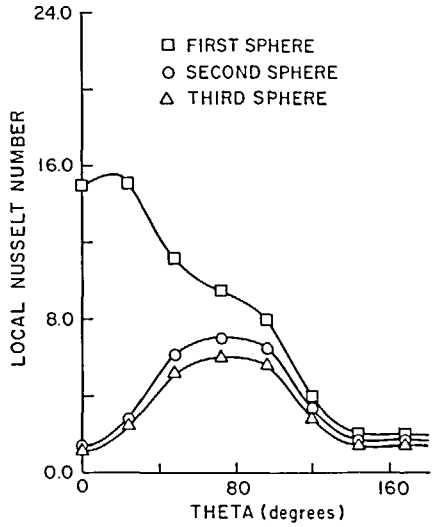

FIG. 10. Local Nusselt number comparison.

The different nature of longitudinal and lateral interactions is most evident when arrays with various longitudinal and lateral spacings are considered. Nusselt number values for the second sphere in a three-sphere cell (being most representative of bulk conditions) are presented in Table 3.

Table 3. Average Nusselt number values for the second of 3 spheres in a cell, $Re = 100$, $Pr = 1$

Lateral spacing	Longitudinal spacing	Nu
1.5	1.5	4.765
1.06	1.5	5.708
1.5	1.35	4.594
1.5	1.2	4.372

CONCLUSIONS

A multisphere cylindrical cell model has been developed for the hydrodynamics and heat transfer in assemblages of spheres. The hydrodynamic solution has been found to be periodic (within a reasonable degree of approximation).

There are trends of decrease in the drag coefficient and in the Nusselt number in the streamwise direction where the definitions of the drag coefficient and of the Nusselt number are based upon the free stream velocity and upon the temperature difference between the inlet and the sphere surface, respectively. Defining the Nusselt number by using average bulk temperature of the cell unit inlet, a periodic result is obtained for the Nusselt number (since the flow field is periodic). However, this periodicity does not imply periodicity in the absolute value of the heat transferred to each sphere.

A solution based on predicting periodicity *a priori* predicts the drag coefficient and Nusselt number with good accuracy. As spacing decreases, the overall heat transfer rates are reduced. This feature is in compliance with the experimental results of Sangiovanni and Labowsky [27], who found a considerable decrease in the rate of vaporization in sprays as compared to single droplets.

In order to predict rates of vaporization in assemblages, the present gaseous-phase analysis will be coupled with the liquid phase of Tong and Sirignano [28] in the near future.

Acknowledgements—The authors gratefully acknowledge the support of the Office of Basic Energy Sciences, and the Pittsburgh Energy Technology Center, Department of Energy.

REFERENCES

1. S. Prakash and W. A. Sirignano, Liquid fuel droplet heating with internal circulation, *Int. J. Heat Mass Transfer* **21**, 885–895 (1978).
2. S. Prakash and W. A. Sirignano, Theory of convective droplet vaporization with unsteady heat transfer in the circulating liquid phase, *Int. J. Heat Mass Transfer* **23**, 253–268 (1980).
3. P. Lara-Urbaneja and W. A. Sirignano, Theory of transient multicomponent droplet vaporization in convective field, in *Proc. 18th Symp. (Int.) on Combustion*. Combustion Institute (1981).
4. N. A. Chigier, The atomization and burning of liquid fuel sprays, *Progr. Energy Combust. Sci.* **2**, 97–114 (1976).
5. G. M. Faeth, Current status of droplet and liquid combustion, *Progr. Energy Combust. Sci.* **3**, 191–224 (1977).
6. N. V. Fedoseeva, Kinetics of evaporization of a droplet system, *Adv. Aerosol Phys.* **3**, 35–42 (1973).
7. E. M. Twardus and T. A. Brzustowski, The interaction between two burning fuel droplets, *5th Int. Symp. on Combustion Processes*, Krakow, Poland, September (1977).
8. M. Labowsky, Calculation of the burning rates of interacting fuel droplets, *Combust. Sci. Technol.* **22**, 217–226 (1980).
9. M. Labowsky, Transfer rate calculations for compositionally dissimilar interacting particles, *Chem. Engng Sci.* **35**, 1041–1048 (1980).
10. M. Labowsky and D. E. Rosner, *Evaporation-Combustion of Fuels, Advances in Chemistry Series*. American Chemical Society, Washington, D.C. (1978).
11. N. V. Fedoseeva, Combustion of a system of liquid fuel drops, *Adv. Aerosol Phys.* **2**, 110–118 (1972).
12. N. V. Fedoseeva, Yu. I. Boiko and A. G. Konyushanko, Evaporization of droplet systems in neutral and chemically active media, *Adv. Aerosol Phys.* **5**, 11–16 (1975).
13. A. K. Ray and E. J. Davis, Heat and mass transfer with multiple particle interactions, Part I. Droplet Evaporation, *Chem. Engng Communications* **6**, 61–79 (1980).
14. H. H. Chiu and T. M. Liu, Group combustion of liquid droplets, *Combust. Sci. Technol.* **17**, 127–142 (1977).
15. R. Tal (Thau) and W. A. Sirignano, Cylindrical cell model for the hydrodynamics of particle assemblages at intermediate Reynolds numbers, *A.I.Ch.E. Jl* **28**, 233–237 (1982).
16. S. Ergun, Fluid flow through packed columns, *Chem. Engng Prog.* **48**, 89–94 (1952).
17. B. P. LeClair and A. E. Hamielec, Viscous flow through particle assemblages at intermediate Reynolds numbers, *I/EC Fundamentals* **7**, 542–549 (1968).
18. R. Tal (Thau) and W. A. Sirignano, Heat transfer in sphere assemblages at intermediate Reynolds numbers: a cylindrical cell model, ASME Paper 81-WA/HT44, 1981 ASME Winter Annual Meeting, Washington, D.C., November (1981).
19. A. S. Gupta and G. Thodos, Direct analogy between mass and heat transfer to beds of spheres, *A.I.Ch.E. Jl* **9**, 751–754 (1963).
20. B. P. LeClair and A. E. Hamielec, Viscous flow through particle assemblages at intermediate Reynolds numbers: heat or mass transport, *Symp. Ser.* **30**, 197–207 (1968).
21. S. W. Woo, Simultaneous free and forced convection around submerged cylinders and spheres, Ph.D. Thesis, McMaster University, Hamilton, Ontario, Canada (1971).
22. T. Akiyama, S. Suzuki and S. Kageyama, Friction factors in the viscous flow through particle assemblages, *J. Chinese Inst. Chem. Engrs* **10**, 1–6 (1979).
23. F. S. Shaw, *An Introduction to Relaxation Methods*. Dover, New York (1953).
24. L. Hageman and D. Young, *Applied Iterative Methods*. Academic Press, New York (1981).
25. S. V. Patankar, C. H. Liu and E. M. Sparrow, Fully developed flow and heat transfer in ducts having streamwise periodic variations of cross-sectional area, *J. Heat Transfer* **99**, 180–186 (1977).
26. R. Tal (Thau), D. N. Lee and W. A. Sirignano, Periodic solutions of heat transfer for streamwise-periodic variations of cross-sectional area (to be published).
27. J. J. Sangiovanni and M. Labowsky, Burning times of linear fuel droplet arrays: a comparison of experiment and theory, *Combustion and Flame* (in press).
28. A. Tong and W. A. Sirignano, Analytical solution for diffusion in the core of a droplet with internal circulation, *20th National Heat Transfer Conference*, Milwaukee, WI, 2–5 August (1982). Also see A. Y. Tong and W. A. Sirignano, *Proc. 19th Symp. (Int.) on Combustion*, Combustion Institute (1983).

HYDRODYNAMIQUE ET TRANSFERT THERMIQUE DANS DES ASSEMBLAGES DE SPHERES—MODELES DE CELLULES CYLINDRIQUES

Résumé—Pour évaluer les intéractions entre des gouttelettes de combustible qui se vaporisent, un modèle de cellule cylindrique basé sur une sphère unique a été proposée par les auteurs dans des travaux antérieurs en remplacement du modèle d'une cellule sphérique. Puisque les effets de sillage sont importants, un modèle cylindrique multisphère est développé ici. Les équations de Navier–Stokes et de l'énergie sont résolues numériquement dans les cellules représentatives pour des nombres de Reynolds intermédiaires. Utilisant une maille non uniforme adaptée au problème, plusieurs sphères en tandem sont considérées et l'importance des effets de sillage dans la réduction, la trainée et de l'effet du nombre de Reynolds est discutée. Les aspects quasipériodiques des résultats sont indiqués et comparés favorablement avec un modèle supposant a priori la périodicité.

STRÖMUNGEN UND WÄRMETRANSPORT IN ANORDNUNGEN VON KUGELN—ZYLINDRISCHES ZELLENMODELL

Zusammenfassung—Um die Wechselwirkungen zwischen verdampfenden Kraftstofftröpfchen zu beschreiben, wurde von den Verfassern in früheren Arbeiten als Ersatz für das bestehende kugelförmige Zellenmodell ein zylindrisches Zellenmodell auf der Grundlage einer Einzelkugel vorgeschlagen. Da die Vorgänge im Nachlauf wichtig sind, wurde in der vorliegenden Arbeit ein zylindrisches Modell für viele Kugeln entwickelt. Die Navier–Stokes- und Energiegleichungen wurden numerisch für die repräsentative Zelle und intermediäre Reynolds-Zahlen gelöst. Mit Hilfe eines dem Problem angepaßten, gleichförmigen Netzes werden verschiedene Kugeln in Tandemanordnung betrachtet und die Bedeutung von Nachlaufeffekten für die erhebliche Verminderung des Widerstandes und der Nusselt-Zahl im Gesamtbereich diskutiert. Die quasiperiodischen Merkmale der Ergebnisse werden aufgezeigt und lassen sich gut mit einem Modell vergleichen, das Periodizität à priori voraussetzt.

ГИДРОДИНАМИКА И ТЕПЛОПЕРЕНОС В СФЕРИЧЕСКИХ СБОРКАХ. МОДЕЛИ ЦИЛИНДРИЧЕСКИХ ЯЧЕЕК

Аннотация—С целью оценки взаимодействий между испаряющимися каплями топлива в предыдущих работах авторов была предложена модель цилиндрической ячейки, расположенной на единичной сфере, вместо ранее используемой модели сферической ячейки. Поскольку большую роль играют эффекты следа, в настоящем исследовании была разработана модель многосферной цилиндрической ячейки. Уравнения Навье-Стокса и энергии решались численно для характерных модельных ячеек при умеренных значениях числа Рейнольдса. Используя соответствующую задаче неравномерную сетку, рассмотрено несколько последовательно соединенных сфер и обсуждено влияние следа на снижение сопротивления и число Нуссельта, осредненное по всей ячейке. Отмечен квазипериодический характер полученных результатов, что выгодно отличается от модели, в которой периодичность принимается априорно.